Robot Design and Testing for Greenhouse Applications

Paolo Gay, P. Piccarolo

Biosystems Engineering

Biosystems Engineering (2006) **95** (3), 309–321
doi:10.1016/j.biosystemseng.2006.07.004
AE—Automation and Emerging Technologies

Robot Design and Testing for Greenhouse Applications

G. Belforte[1]; R. Deboli[2]; P. Gay[3]; P. Piccarolo[3]; D. Ricauda Aimonino[3]

[1]DAUIN, Politecnico di Torino, 24 Corso Duca degli Abruzzi, 10129 Torino, Italy; e-mail: gustavo.belforte@polito.it
[2]CNR, IMAMOTER, 73 Strada delle Cacce, 10135 Torino, Italy; e-mail: r.deboli@imamoter.cnr.it
[3]DEIAFA, Università degli Studi di Torino, 44 Via Leonardo da Vinci, 10095 Grugliasco (TO), Italy; e-mail of corresponding author: paolo.gay@unito.it

(Received 9 November 2005; accepted in revised form 13 July 2006; published online 20 September 2006)

The latest results of technology and research are increasingly used in agriculture, especially in intensive cultures that ensure remunerative returns. Most cultures in greenhouses are in this category where, despite the large use of technology, human operators still manually perform most operations on the crop although they are often highly repetitive and sometime even dangerous. This fact greatly impacts on the quality of the product, on the production costs and on collateral issues, such as pollution and safety. In this paper, the state of research in robotic automation in agriculture outlining the characteristics that robots should have to allow their profitable use is considered. A multi-purpose low-cost robot prototype, designed and built according to such characteristics, is then presented together with the results of some preliminary experimentation with it. Although more research is needed, the results prove to be promising and show some advantages that can be achieved with robotic automation. In particular, precision spraying and precision fertilisation applications have been developed and tested. Although the productivity of the prototype is quite low (in the range of 400–500 plant/h), experiments conducted continuously for several hours show that the robot can perform tasks unaffordable by human operators.

1. Introduction

In recent decades, advanced technology and latest results of scientific research have been largely applied in agriculture in order to improve the quality of products and to increase the productivity. A typical example for illustrating this trend is the wide use of genetic manipulation for creating hybrids species of flowers (or other plants) with special characteristics that fit the need of the market and allow better economic returns. Another example is given by the climatic control usually implemented in greenhouses that can range from relatively simple solutions regulating temperature and humidity to very sophisticated (and expensive) where even the temperature of the soil is controlled, heating or cooling it in order to induce blooming in some flower species.

In this framework in which innovative technologies are widely used and accepted for some aspects of the production cycle, it is remarkable to note that agriculture is still very labour intensive even in the western countries where cost of manpower is very high and automation strategies have not yet found an extensive application comparable with the one that can be found in other industrial sectors.

Indeed, some research work has been done and some applications are available as illustrated in Kondo and Ting (1998), but most developed solutions are focused on specific problems and single applications.

In order to provide a short overview of the literature evidencing the main applications that have been investigated and the solutions that have been proposed, it is convenient to distinguish between studies devoted to applications in the field and those foreseen for the protected environment in greenhouses.

For applications in the field, consistent efforts have been devoted to the study of automatic guidance systems for tractors as well as for other specific machines such as

Notation

$\boldsymbol{A}_{i-1,i}$	transformation matrix relative to the $(i-1)$th and ith coordinate systems	$\boldsymbol{T}_{x,\alpha}$	transformation matrix describing the rotation around the X axis
a_i	physical dimension of the ith joint: minimum distance (if any) between Z_{i-1} and Z_i measured in the X_i direction	$\underline{u}_i, \bar{u}_i$	lower and upper bounds of the ith input command
b	physical dimension of the mechanical structure (see *Fig. 4* for more details), mm	u_1, u_2, u_3	input command of the joint 1,2,3, respectively
c	length of the actuator of joint 1, mm	W	set of points that can be reached by the end-effector of the robot
c_0	length of the actuator of joint 1 when it is fully contracted, mm	$\hat{\boldsymbol{x}}_i, \hat{\boldsymbol{y}}_i, \hat{\boldsymbol{z}}_i$	set of unit vectors defining the $(i+1)^{\text{th}}$ joint
d_i	longitudinal displacement of the ith joint, mm	X_i, Y_i, Z_i	axes of the $(i+1)^{\text{th}}$ joint
$F(u_1,u_2,u_3)$	the direct kinematics function	x_i,y_i,z_i	x,y,z coordinates expressed according to the $(Oxyz)_i$ reference system
f	length of the actuator of joint 2, men	α_i	physical dimension of the ith joint: angle between Z_{i-1} and Z_i around the X_i axis
f_0	length of the actuator of joint 2 when it is fully contracted, mm	β	angle generated by the actuator of joint 1, deg
g	physical dimension of the mechanical structure (see *Fig. 5* for more details), mm	β_0	angle generated by the actuator of joint 1 when it is fully contracted, deg
h	physical dimension of the mechanical structure (see *Fig. 5* for more details), mm	δ	angle generated by the actuator of joint 2 (See *Fig. 5* for more details), deg
k_1,k_2,k_3	mechanical gain of the joint 1,2,3, respectively	λ, γ	angles of the mechanical structure (see *Fig. 5* for more details), deg
$(Oxyz)_0$	inertial reference system	e	physical dimension of the mechanical structure (see *Fig. 4* for more details), mm
$(Oxyz)_i$	reference system of the $(i+1)^{\text{th}}$ joint	θ_i	rotation angle of the ith joint, deg
p_i	generic point in the space referred to the coordinate system of the ith joint	ρ	net angle generated by the actuator of joint 1, deg
r	physical dimension of the mechanical structure (see *Fig. 4* for more details), mm	φ	angle generated by the actuator of joint 2, deg
$\boldsymbol{T}_{z,d}$	transformation matrix describing the displacement along the Z axis	φ_0	angle generated by the actuator of joint 2 when it is fully contracted, deg
$\boldsymbol{T}_{z,\theta}$	transformation matrix describing the rotation around the Z axis	Ω	set of all possible input commands to the joints
$\boldsymbol{T}_{x,\alpha}$	transformation matrix describing the displacement along the X axis		

harvesters, transplanters, *etc*. Different technological solutions have been suggested. Some make use of global navigation satellite systems (GNSS) presently represented by the American global positioning system (GPS) (see *e.g*. Thuilot *et al.*, 2001; Bak & Jakobsen, 2004), while others are based on artificial vision as in the works of Hague and Tillett (1996), Hague *et al.* (2000), Marchant *et al.* (1997), Åstrand and Baerveldt (2002) and Tillett (1991). In this last context, a special section concerns applications based on stereoscopic vision as in the works of Kise *et al.* (2005) and Rovia Màs *et al.* (2004). The use of GPS and artificial vision have been combined together by Benson *et al.* (2003) and Chen *et al.* (2003), while solutions based on ultrasonic sensing (Harper & Mc Kerrow, 2001) and lasers (Jimenez *et al.*, 1999; Château *et al.*, 2000) have been also proposed.

Beside guidance problems, automated solutions have been studied for specific cultural operations such as the automatic hoe control (Tillett & Hague, 1999), the inter-row raking and tilling for weed control in sugar beet (Tillett *et al.*, 2002; Åstrand & Baerveldt, 2002).

Automated weed control implemented with electrical discharges has been studied by Blasco *et al.* (2002) while the problem of precision spraying for weed control has been addressed by Tian *et al.* (1999) and Paice *et al.* (1995), and in Tillett *et al.* (1998) precision spraying is considered for crop treatment.

Final fields of study for automated applications in the field are represented by robotic solutions for harvesting,

as illustrated by the works of Monta *et al.* (1995), Sarig (1993), Sanders (2005) and Peterson *et al.* (1999), and mapping yield and fruit quality (Qiao *et al.*, 2005).

Also with respect to the automated solutions for application in greenhouses, the main lines of study concern guidance problems, specific cultural operations and harvesting. In Mandow *et al.* (1996) and Sandini *et al.* (1990), the focus is on guidance of robots in greenhouses, while Tillett (1993) offers an excellent overview in robotic applications in horticulture. Automated cucumber picking by a robot was studied by Van Henten *et al.* (2002, 2003), while Reed *et al.* (2001) address the automatic harvesting of cultivated mushrooms. Cho *et al.* (2002) consider a lettuce harvesting robot with computer vision and Kondo and Monta (1999) present strawberry harvesting robots. Other cultural operations whose automation has been specifically studied are transplanting and seeding as in the works of Ryu *et al.* (2001) and of Tai *et al.* (1994).

It is worth noting that most solutions presented in the literature deal with the automation of specific agricultural operations for which dedicated machines are designed and tested. Such machines can be quite complex and sophisticated but from the very beginning they are developed for a particular application only. The case of studies involving multi-purpose flexible robots that can perform different tasks on the crop is an exception. Some interesting works in this category are those of Monta *et al.* (1995), and of Van Henten *et al.* (2002, 2003, 2004).

Despite the fact that multi-purpose robots for agricultural applications have not been studied much so far, the development of this kind of machines could represent, especially for cultivations in greenhouses, a valid solution for several problems and could be strategic in order to improve the competitiveness of the horticultural and flower producers.

It is convenient to analyse the several reasons for which it is suggested that, at least in a first stage, robots are designed for operating in greenhouses, while the possible extension of their use to the field is left for the future. Such reasons can be grouped in three main categories: technical, economic, and social/environmental. Technical reasons are related to the fact that greenhouses are an environment in which some functions such as irrigation, light and temperature control are already automatically performed; thus, the introduction of multi-purpose robots represents a further development in their automation. Greenhouses represent a rather structured environment that consequently facilitates robotic applications: surfaces are more regular than in the field and the position of the plants (which are the target of the operations) are at least partially known. Available power supply and the same structure of the greenhouse can facilitate the installation of the new equipment and reduce installation costs since the navigation of the robot could be ensured using rails, easy to be installed on the floor, or hooked to the plinths, or the robot could work in fixed position coupled with moving benches lines, when these last are available. Economic reasons are related to the fact that greenhouses are anyway quite expensive facilities where in general highly remunerative crops are intensively grown. This fact indeed can justify and facilitate new consistent investments (Sandini *et al.*, 1990). Moreover the introduction of robotic operations in greenhouses should increase the productivity and the quality of production for two main reasons: firstly it would reduce the need of manpower for several repetitive and tedious operations; secondly, it would permit mechanically performing some operations (as for example precise spraying) that cannot be done routinely by human operators since they are too time consuming or too demanding in terms of concentration of the operator. Finally, the possibility of tending automatically each plant could allow new protocols for precise spraying and fertilisation that could reduce the amount and consequently the cost of used chemicals. This last consideration introduces the social and environmental advantages that could be secured by the use of robots in greenhouses. Repeated sessions of pesticide and herbicide spraying are required in greenhouses since the favourable climate created for optimal plant growth and the intensive cultivation cause undesirable organisms and pest to prosper. Automated spraying sessions could be better controlled and avoid the involvement of human operators. This would result in a reduction of environmental pollution, in less risks, and less work illnesses as well as in an increased quality of the working environment for all relevant operators.

The natural question that arises from the above consideration is: why has robotic automation not yet been introduced in agriculture? Kassler (2001) discusses factors that have prevented or retarded the exploitation of computer-controlled machines in agriculture. They can be summarised as: insufficiently robust and costly mechanical technology, limited working capability of the machine and currently insufficient available knowledge to create robots as dexterous or as skilful as a trained worker. Moreover, as pointed out before, most available automated machines are able to perform a single specific agricultural task. Since the seasonality of most agricultural production imposes the use of the machine for only a few times per year, this increases the costs that cannot be reduced by sharing the machine with other farmers because neighbourhood properties usually follow the same calendar and need the machine at the same time.

From this analysis, the main obstacle to the introduction of robotic solutions in agriculture seems to be related to the fact that commercially available equipment does not fit with the needs of the operators. However, in our opinion, the technology is mature for producing innovative machines that can be really useful and economically sounded for the market.

2. Important features and requirements for robots in a greenhouse

In the following, the characteristics of commercial robots intended for operating in greenhouses are discussed. Such characteristics have been the main guidelines for the development of the prototype described in this paper.

The first important consideration concerns the precision requirements for a robot designed to work in greenhouses and perform agricultural operations. It is evident that errors and uncertainties in the order of some millimeters are acceptable for almost any agricultural operation. This implies that the accuracy error, for this kind of robot, is about two to three orders of magnitude greater than the that expected for commercial robots in industrial environments. This fact has a great impact on the design since less precision implies looser constraints on the quality of the components to be used as well as on the design of the mechanical structure that does not need to be very rigid but can allow some deformation. All this, obviously, results in lower weight and particularly in lower production costs that turn into a lower final price for the robot.

The greenhouse environment is humid and dirty with possible spraying of chemicals. The workers that will use and routinely take care of the machine will in general not have specific competences on robots. The robot structure should therefore be designed taking this facts into account. Simple structures based on standard commercial components, beside contributing to the general cost reduction, are usually more robust and easy to maintain.

Although greenhouses can be considered as partially structured environments, nonetheless they are far away from the levels that can be typically found in industrial environments such as assembly lines where robotic cells are widely used. Solutions to take care of this problem with proper sensors should be carefully considered. Probably the availability of an artificial vision system that can be used to identify obstacles or targets whose position and/or shape is not always perfectly known is the most convenient solution. This is also because an artificial vision system can be used for other tasks such as inspection and growth evaluation of each single plant. It is, however, important to use the structure of the environment as much as possible and increase it whenever this is feasible and leads to simpler solutions. In this connection, it is strongly recommended that layout design and operation planning are oriented to minimise (or to exclude) the autonomous navigation of the robot inside the greenhouse since this feature is complex and requires huge computational resources while a rail (or similar system) can greatly simplify the task (and the costs).

The surface in the greenhouse is exploited to the largest possible extent due to the high costs of the structure. For this reason, it is important that the robot is as little demanding as possible in terms of the space that it diverts from the productive activity. A cumbersome machine must be carefully avoided. Similarly, it is recommended that the total weight of the robot is restricted. This is important to allow more flexible use of the machine that is less demanding in terms of the infrastructure (such as rails for its movement) required for its use because robot design should be compatible with existing structures, as well as accommodating scaling in size and operating volume to adapt to different existing conditions.

A very important feature is the versatility of the robot to undertake a range of agricultural operations with easy conversion from one operation to another. In this way it could be possible to (almost) automate the entire growth and production cycle of some cultivations, making the robot more appealing. Obviously each elementary operation should be done in the shortest possible time.

Finally the cost of the robot should be as low as possible.

It is worth noting that the features discussed so far clearly show fundamental differences between the characteristics required for robots to be used in agriculture and those required for robots to be used in manufacturing applications. This consideration implies that the use of commercially available robots, that at present are all designed for manufacturing applications, is not advisable for applications in agriculture. New machines should instead be designed and produced to better fit the specific needs of the sector. To allow this to happen, specific robot prototypes should be built and used to facilitate experiments and research on different complementary aspects of automation in agriculture with a special focus on greenhouses. As research tools these robots do not need to satisfy all the constraints required for a commercial product (in terms of costs, simplicity, performances, *etc.*) since these topics can be delegated to a future engineering phase.

3. Specifications and features of the prototype robot

A prototype robot was built in the framework of a cooperative study undertaken by a team of Italian research institutions comprising the Dipartimento di Economia e Ingegneria Agraria Forestale e Ambientale of the Università degli Studi di Torino, the IMAMOTER laboratories of the Consiglio Nazionale delle Ricerche, and the Dipartimento di Automatica e Informatica of the Politecnico di Torino.

Since the robot was the first prototype to be constructed by the research team, it was decided to keep it as simple as possible in order to reduce the costs of this first trial but nevertheless include enough features to support valuable research. For this reason, the degrees of freedom were limited to three (the minimum requirement for significant experiments); no movement within the greenhouse was foreseen since this is not essential for conducting experiments and can be added subsequently (or the robot can be combined with mobile benches). A few operations with the robot were foreseen but no special care has been devoted to the way in which different tools can be easily secured to the end-effector since this problem can be delegated to an engineering phase. Similarly, no requirements were set for the velocity at which the machine can operate. On the contrary, the robot kinematics was required to allow to operate on a surface of at least 1–2 m^2 ensuring at the same time a minimum encumbrance. Finally, the robot was equipped with a simple vision system since this seems to be an unavoidable requirement to properly operate in a incompletely structured environment in which functions of monitoring and inspection are also an objective. The robot was constructed with standard components available on the market and with simple home-built parts that did not require particular processing. The result of the design is presented in the following section.

Fig. 1. The robot operating in the greenhouse

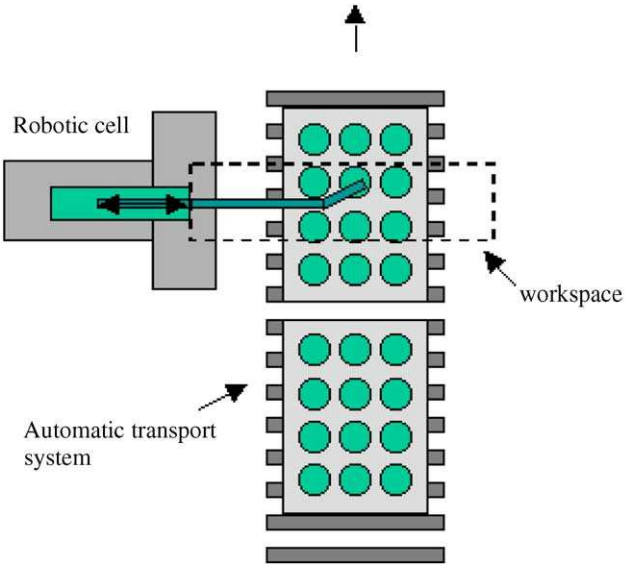

Fig. 2. Layout of the robot cell in the greenhouse with the bench displacement system

4. Mechanical design and kinematics

The robot presented in this paper was designed to operate in a fixed position in the greenhouse. It was interfaced to a standard belt-conveyor displacement system that provides the robot with pallets containing the crops, usually grown in pots.

The robot consists of a three degrees of freedom manipulator that can be equipped with different end-effectors and tools adding further degrees of freedom to the system (*Fig. 1*). Its reachable working space can be well approximated by a rectangular shaped box placed across the conveyor line (*Fig. 2*).

The longitudinal movement, orthogonal to the moving direction of pallets and benches, is performed by a pantograph mechanical structure that reduces the back side play. This is particularly important in connection with the high exploitation of the greenhouse soil surface imposed by economic considerations that require the limitation of the overall side play of the manipulator in order to reduce unproductive volumes within the greenhouse.

The kinematic chain generating the longitudinal displacement d_1 of 1680 mm has been modelled as a prismatic joint (see joint 1 in *Fig. 3*). The second joint, that allows a rotation of an angle θ_2 of about $\pm 50^\circ$, is connected to a frame whose length a_2 is 390 mm.The

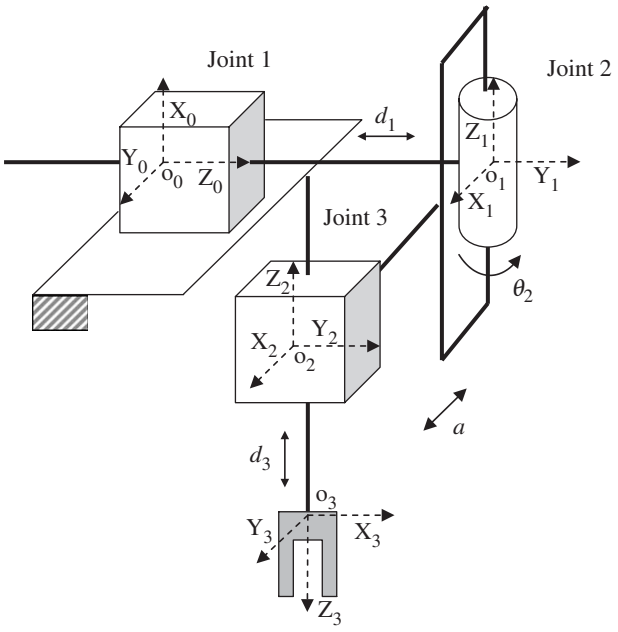

Fig. 3. Kinematic equivalent model of the manipulator. The non-constant parameters identifying each link are evidenced as follows: d_1, longitudinal displacement; d_3, vertical range; a_2, frame length; θ_2, rotation angle. The values of the constant parameters identifying each link are reported in Table 1

third joint is prismatic and it operates along the vertical direction, with a range d_3 of 400 mm.

All joints are driven by endless screws coupled with 12 V DC motors. The position of the linear actuators are measured by two potentiometers (joints 2 and 3) and by a digital encoder (joint 1).

From an analytical point of view, the manipulator can be described by an equivalent kinematic chain of rigid arms linked together by joints with one degree of freedom, the first arm of the kinematic chain being connected to the reference frame.

A convenient description of the kinematic chain with its rotations and translations can be obtained by applying the notation of Denavit and Hartemberg (1955), that allows the analytical derivation of a coordinate reference system for any link of the chain. According to this notation independent reference coordinate systems are associated to each rigid body representing the different links of the robot. The rule for choosing the orientation of each coordinate system is reported below.

The action of any joint is then described by a quaternion transformation matrix that expresses translations and rotations by means of homogeneous transformations. The complete kinematic chain can be formalised as the application of a sequence of homogeneous transformation matrices. The coordinates of the end-effector and eventually of the targets when expressed according to a reference system associated with the tool handler (the hand reference), can be easily rewritten with respect to the inertial (reference) coordinate system aligned with the frame of the steady part of the robot.

The rule for choosing the axes orientation is now described. Let $(Oxyz)_0$ be the inertial reference coordinate system of the frame of the robot. To describe the kinematic chain introduce n orthonormal coordinate systems $(Oxyz)_i$, $i = 1, \ldots, n$, where n is the number of degrees of freedom of the manipulator (in our case $n = 3$). Each coordinate system $(Oxyz)_i$, $i = 1, \ldots, n$, is associated with the $(i+1)^{\text{th}}$ link and its three unit vectors $\{\hat{x}_i, \hat{y}_i, \hat{z}_i\}$ are chosen as follows:

(a) axis Z_{i-1} lies along the direction of movement or rotation of the ith joint and, in the case of rotation joint, the orientation is chosen according to the right-hand-rule;
(b) axis X_i is orthogonal to the Z_{i-1} and Z_i axes;
(c) axis Y_i is chosen in order to obtain a right-handed coordinate system.

When the ith joint is activated, link ith (and its related coordinate system) moves with respect to the $(i-1)$th link. Therefore the ith coordinate system can be expressed according to the reference coordinate system $(Oxyz)_0$ by the knowledge of the $(Oxyz)_k$, $k = 1, \ldots, i-1$, intermediate coordinate systems.

In *Fig. 3* the kinematic diagram of the manipulator together with its coordinate reference systems are reported. Note that, while joint 3 is directly implemented by an endless screw actuator, joints 1 and 2 are implemented with a composite mechanical structure described in the following.

Each link is identified in general by four parameters a_i, α_i, d_i, θ_i whose values and variability depend on the structure of the specific link under consideration. Note that for each specific link structure some of the parameters are in general constant and correspond to specific physical dimensions. The parameter a_i represents the minimum distance (if any) between Z_{i-1} and Z_i measured in the X_i direction; α_i is the angle between Z_{i-1} and Z_i around the X_i axis (the positive direction is given by the right-hand rule). The distance d_i is evaluated between the origin of the $(i-1)$th coordinate system and the intersection of Z_{i-1} with X_i measured along Z_{i-1} and θ_i is the rotation angle of the joint from X_{i-1} to X_i, around Z_{i-1} (again the positive direction is given by the right-hand rule).

Note that parameters a_i and α_i describe the structure of the link, while d_i and θ_i the relative position of the joint with respect to the adjacent links. According to the

Table 1
Parameters of the three links of the manipulator

Link (i)	θ_I, *deg*	α_I, *deg*	α_i, *m*	d_i, *m*
1	90	90	0	d_i
2	θ_2	0	a_2	0
3	90	180	0	$-d_3$

previous consideration, the parameters of the three links of the specific manipulator under study are reported in Table 1.

When a Denavit and Harteberg representation is used with proper coordinate systems for each link, an homogeneous matrix transformation $\boldsymbol{A}_{i-1,i}$ relating the $(i-1)$th and ith coordinate systems can be derived. Such a matrix describes the two rotations and the two translations into which any possible relative displacement between two adjacent links can be decomposed.

Each of the these four basic movements can be expressed by means of convenient transformation matrices $\boldsymbol{T}_{z,d}$, $\boldsymbol{T}_{z,\theta}$, $\boldsymbol{T}_{x,a}$, $\boldsymbol{T}_{x,\alpha}$, so that their product lead to $\boldsymbol{A}_{i-1,i}$ as follows:

$$\begin{aligned}\boldsymbol{A}_{i-1,i} &= \boldsymbol{T}_{z,d}\boldsymbol{T}_{z,\theta}\boldsymbol{T}_{x,a}\boldsymbol{T}_{x,\alpha}\\ &= \begin{bmatrix}1&0&0&0\\0&1&0&0\\0&0&1&d_i\\0&0&0&1\end{bmatrix}\begin{bmatrix}\cos\theta_i&-\sin\theta_i&0&0\\\sin\theta_i&\cos\theta_i&0&0\\0&0&1&0\\0&0&0&1\end{bmatrix}\\ &\times\begin{bmatrix}1&0&0&a_i\\0&1&0&0\\0&0&1&0\\0&0&0&1\end{bmatrix}\begin{bmatrix}1&0&0&0\\0&\cos\alpha_i&-\sin\alpha_i&0\\0&\sin\alpha_i&\cos\alpha_i&0\\0&0&0&1\end{bmatrix}\\ &= \begin{bmatrix}\cos\theta_i&-\cos\alpha_i\sin\theta_i&\sin\alpha_i\sin\theta_i&a_i\cos\theta_i\\\sin\theta_i&\cos\alpha_i\cos\theta_i&-\sin\alpha_i\cos\theta_i&a_i\sin\theta_i\\0&\sin\alpha_i&\cos\alpha_i&d_i\\0&0&0&1\end{bmatrix}\end{aligned} \tag{1}$$

Any point $p_i = (x_i, y_i, z_i, 1)^{\mathrm{T}}$, represented according to the coordinate system of the ith link can then be expressed according to the coordinate system of the $(i-1)$th link by

$$p_{i-1} = \boldsymbol{A}_{i-1,i}p_i \tag{2}$$

It follows that the representation with respect to the inertial coordinate system $(\mathrm{O}xyz)_0$ is given by

$$p_0 = \prod_{k=1}^{i}\boldsymbol{A}_{k-1,k}p_i \tag{3}$$

The derivation of the matrices $\boldsymbol{A}_{0,1}$, $\boldsymbol{A}_{1,2}$, and $\boldsymbol{A}_{2,3}$ for the specific case of the robot described within this paper has been reported in Appendix A.

Applying to our robot relation (3) with $i = 3$, it follows that:

$$\begin{pmatrix}x_0\\y_0\\z_0\\1\end{pmatrix} = \begin{bmatrix}0&0&-1&-d_3\\-\sin\theta_2&\cos\theta_2&0&a_2\cos\theta_2\\\cos\theta_2&\sin\theta_2&0&a_2\sin\theta_2+d_1\\0&0&0&1\end{bmatrix}\begin{pmatrix}x_3\\y_3\\z_3\\1\end{pmatrix} \tag{4}$$

Such a matrix relation can be expanded into the following set of three independent equations:

$$\begin{cases}x_0 &= -z_3 - d_3\\ y_0 &= -x_3\sin\theta_2 + y_3\cos\theta_2 + a_2\cos\theta_2\\ z_0 &= x_3\cos\theta_2 + y_3 sin\,\theta_2 + a_2\sin\theta_2 + d_1\end{cases} \tag{5}$$

Assuming, without loss in generality, that the end-effector is in the origin of the coordinate system $(\mathrm{O}xyz)_3$ (relative to the third joint) so that $x_3 = y_3 = z_3 = 0$, it follows that:

$$\begin{cases}x_0 &= -d_3\\ y_0 &= a_2\cos\theta_2\\ z_0 &= a_2\sin\theta_2 + d_1\end{cases} \tag{6}$$

With the particular mechanical structure of the joints 1 and 2, in the robot under consideration the parameters d_1 and θ_2 characterising the two links cannot be directly controlled. In the following, the two kinematics chains that implement movements of these two joints are analysed.

Concerning joint 1, whose structure is reported in *Fig. 4*, the relations linking the displacement d_1 to the length c of the linear actuator moving the joint are:

$$c_0^2 = e^2 + b^2 - 2eb\cos(\beta_0) \tag{7a}$$

$$c^2 = e^2 + b^2 - 2eb\cos(\beta) \tag{7b}$$

where c, β, e and b are physical dimensions of the mechanical structure of the robot described in *Fig. 4* and c_0 and β_0 are the values of c and β when the actuator of joint 1 is fully contracted.

Defining $\rho = \beta - \beta_0$, Eqn (7b) can be rewritten as:

$$c^2 = e^2 + b^2 - 2eb\cos(\beta_0 + \rho) \tag{8}$$

so that the equivalent longitudinal displacement d_1 can be derived as

$$d_1 = 2r\sin(\rho) \tag{9}$$

where the angle ρ, resulting from Eqn (8), is

$$\rho = \arccos\left(\frac{e^2 + b^2 - c^2}{2eb}\right) - \beta_0 \tag{10}$$

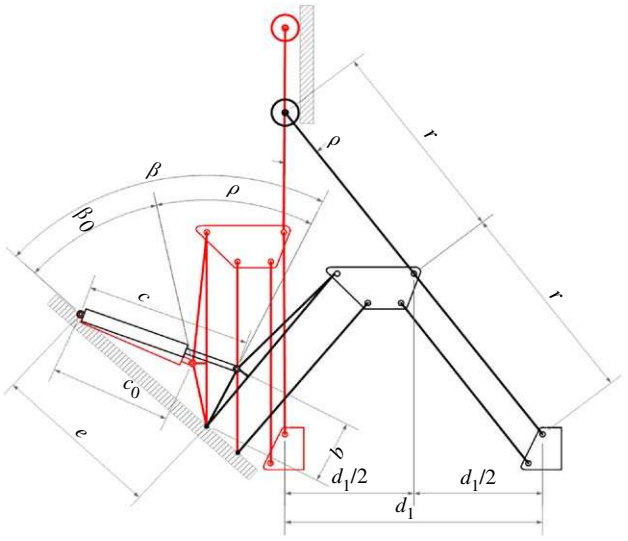

Fig. 4. Mechanical structure of the equivalent joint 1; the actual dimension for this part of the manipulator are $b = 300\,mm$, $c_0 = 460\,mm$, $e = 740\,mm$, $r = 900\,mm$ *and* $\beta_0 = 19^\circ$

From Euler's theorem the inequalities

$$-1 \leqslant \frac{e^2 + b^2 - c^2}{2eb} \leqslant 1 \tag{11}$$

hold true so that $-2eb \leqslant e^2 + b^2 - c^2$ and $e^2 + b^2 - c^2 \leqslant 2eb$.

Note that the length c of the actuator of joint 1 can be written as

$$c = c_0 + k_1 u_1 \tag{12}$$

where k_1 and u_1 are respectively the mechanical gain and the angular position in the endless screw device implementing the actuator.

Concerning joint 2, whose structure is shown in *Fig. 5* the rotation angle θ_2 is

$$\theta_2 = \delta - \frac{\pi}{2} \tag{13}$$

where δ is the angle reported in the same figure. Note that δ can be expressed as

$$\delta = \varphi + \lambda + \gamma \tag{14}$$

where φ, λ, and γ are the angles shown in *Fig. 5*.

Again, using the Carnot's relations:

$$f_0^2 = g^2 + h^2 - 2gh\,\cos\varphi_0 \tag{15a}$$

$$f^2 = g^2 + h^2 - 2gh\,\cos\varphi \tag{15b}$$

where f, g, and h are physical dimensions of the mechanical structure of joint 2 described in *Fig. 5* and φ_0 and f_0 are the values of φ and f when the joint is fully contracted.

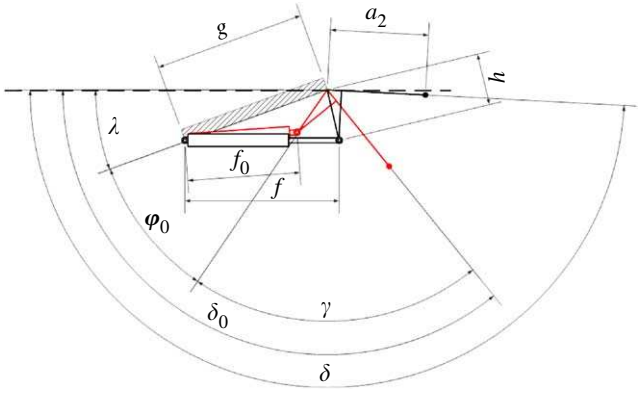

Fig. 5. Mechanical structure of the equivalent joint 2; the actual dimensions are: $a_2 = 390\,mm$, $f_0 = 460\,mm$, $g = 600\,mm$, $h = 200\,mm$, $\lambda = 20^\circ$, $\gamma = 74^\circ$ *and* $\varphi_0 = 38^\circ$

Then φ can be expressed as:

$$\varphi = \arccos\left(\frac{g^2 + h^2 - f^2}{2gh}\right) \tag{16}$$

Noting that:

$$-1 \leqslant \frac{g^2 + h^2 - f^2}{2gh} \leqslant 1 \tag{17}$$

results in $-2gh \leqslant g^2 + h^2 - f^2$, and $g^2 + h^2 - f^2 \leqslant 2gh$.

The length f of the linear actuator moving the joint can be expressed as

$$f = f_0 + k_2 u_2 \tag{18}$$

where k_2 is the mechanical gain and u_2 the command of the actuator.

Substituting Eqns (9) and (13) into (6) with some algebraic manipulations it follows:

$$\begin{cases} x_0 &= -d_3 \\ y_0 &= a_2 \sin\,\delta \\ z_0 &= 2r \sin\,\rho - a_2 \cos\,\delta \end{cases} \tag{19}$$

and provides the position of the end-effector with respect to the coordinate system $(Oxyz)_0$ as a function of δ and ρ (as well as the vertical range d_3).

Let d_3 be described as:

$$d_3 = k_3 u_3 \tag{20}$$

where k_3 and u_3 are, respectively, the mechanical gain and the command of the liner actuator of the third link.

Using Eqns (10) and (12) as well as Eqns (14), (16) and (18) to express the dependence of ρ and δ over the actual inputs u_1 and u_2 acting on joints 1 and 2 and using Eqn (20) to express the dependence of joint 3 from input

u_3, Eqn (19) can be rewritten as:

$$\begin{cases} x_0 = -d_3 = -k_3 u_3 \\ y_0 = a_2 \sin\left(\arccos\left(\dfrac{g^2 + h^2 - (f_0 + k_2 u_2)^2}{2gh}\right) + \lambda + \gamma\right) \\ z_0 = 2r \sin\left(\arccos\left(\dfrac{e^2 + b^2 - (c_0 + k_1 u_1)^2}{2eb}\right) - \beta_0\right) \\ \qquad -a_2 \cos\left(\arccos\left(\dfrac{g^2 + h^2 - (f_0 + k_2 u_2)}{2gh}\right) + \lambda + \gamma\right) \end{cases} \tag{21}$$

The workspace W is the set of points that can be reached by the end-effector of the robot and, it can be expressed as:

$$W = \{q \in \mathbf{R}^3 : q = F(u_1, u_2, u_3), (u_1, u_2, u_3) \in \Omega\} \tag{22}$$

where

$$\Omega = \{(u_1, u_2, u_3) \in \mathbf{R}^3 : \underline{u}_i \leqslant u_i \leqslant \bar{u}_i, i = 1, \ldots, 3\} \tag{23}$$

is the set of all possible input commands to the joints, F being the direct kinematics function described by relation (21) and $\underline{u}_i$and $\bar{u}_i$ are the lower and upper bounds of the input commands.

The workspace was evaluated by simulation using Matlab® and the nominal parameters of the robot and it is reported in *Fig. 6*.

To operate a robot, however, it is necessary to derive its inverse kinematics in which the robot commands are expressed as function of the coordinates of the end-effector. This because in practical applications it is known where, within the working space, the end-effector must move and the commands ensuring such movement must be derived.

The inverse kinematic derivation is a quite complex task since, in general, it does not have a unique solution. In the present case, owing to the simple mechanical structure of the manipulator, the kinematics are fully invertible and can be derived by inverting the set of Eqn (21). With some straightforward algebra, it results that:

$$\rho = \arcsin\left(\frac{z_0 + a_2 \cos\delta}{2r}\right) \qquad \delta = \arcsin\left(\frac{y_0}{a_2}\right) \tag{24}$$

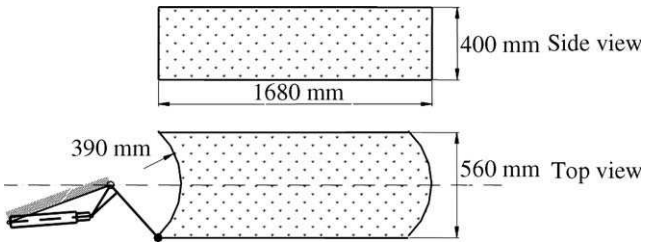

Fig. 6. The numerical simulation of the achievable workspace

and

$$f = \sqrt{g^2 + h^2 - 2gh\cos(\delta - \lambda - \gamma)}$$
$$c = \sqrt{e^2 + b^2 - 2eb\cos(\beta_0 + \rho)} \tag{25}$$

and, finally:

$$\begin{cases} u_1 = -c_0 \\ \qquad + \sqrt{e^2 + b^2 - 2eb\left(\beta_0 + \arcsin\left(\dfrac{z_0 + a_2 \cos\left(\arcsin(y_0/a_2)\right)}{2r}\right)\right)} \\ u_2 = \dfrac{-f_0 + \sqrt{g^2 + h^2 - 2gh\,\cos\left(\arcsin\left(\frac{y_0}{a_2}\right) - \lambda - \gamma\right)}}{k_2} \\ u_3 = \dfrac{x_0}{k_3} \end{cases} \tag{26}$$

The mechanical structure has been implemented using standard steel tubes with square and rectangular hollow sections 3 mm thick. In more detail, for the pantograph structure of the first axis, 50 mm by 50 mm square hollow section was used together with brass and steel pivots. Other structural elements were manufactured using 60 mm by 20 mm rectangular hollow section. The third axis was implemented using a steel cylindrical bar with an axial bearing. In order to compensate for the destabilising momentum generated by the extension of joint 1, 80 kg of iron ballast was added to the rear of the robot.

5. Axis motion and control

The robot control logic was implemented in a control unit mainly comprising a National Instrument 1000b PXI controller equipped with a PXI-8170 Pentium III central processing unit (CPU) board and a PXI-7344 motion controller.

The three joints described in the above section are actuated by three endless screw 12 V DC motors. Each motor is powered by a pulse width modulation (PWM) driver which also controls the velocity of the joint, with the armature voltage feedback. The actuator of the joint 1 is equipped with a digital encoder, while motors of joints 2 and 3 are connected to two potentiometers.

The PWM amplifiers are driven by the digital axes controller on the 7344 board. The position measurements of the three axes are fed-back to the digital PID controllers of the 7344 board.

A digital video camera (JAI S3200) has been connected to the second joint in order to maintain a constant altitude from the bench (see *Fig. 7*). For calibration purposes, a laser pointer has been placed near the camera. Images of the workspace and targets

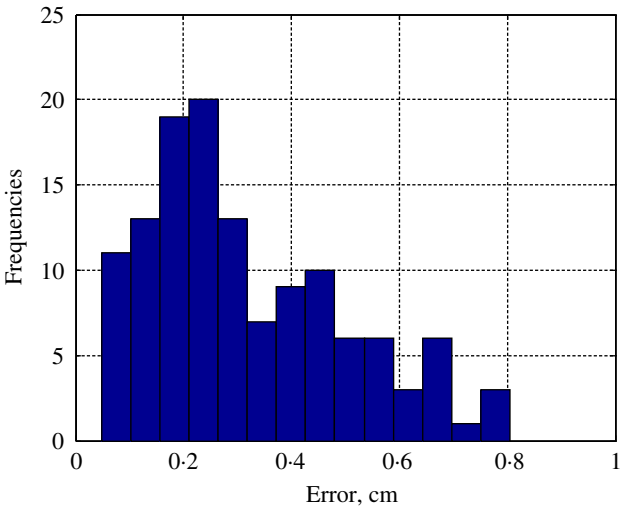

Fig. 7. Histogram of the absolute error reported after the correction

are acquired by the PXI-7411 board at a typical rate of 30 frames per second.

The software of the control unit has been developed using LabView®6 together with the IMAQ® and Flexmotion® libraries and performs different tasks in parallel: trajectory generation, target or obstacle detection, tracking, elaboration of images from the charge coupled device (CCD) camera.

The core of the code is dedicated to the coordination of motion of the three axes with respect to the external events that could occur (target or obstacle detection, tracking during operations, *etc.*). This component of software includes the generation of the trajectories in the workspace, the computation of the single joint trajectories using the inverse kinematics relations and the interface to the 7344 board.

A second block of code is dedicated to the acquisition and the elaboration of the images arising from the colour CCD camera. Images are used to detect and locate targets crops and pots in the working space and to generate the robot trajectories accordingly. A detailed description of the algorithms implemented for image elaboration and plant detection can be found in Gay and Giglio (2003).

6. Calibration, error analysis and experimental results

The positions of the three linear actuators moving the three joints of the robot are measured through two potentiometers and one digital encoder as previously described. These measurements are fed back to the robot control unit and used for control purposes. Note that the actual position of the end-effector in the working space is not directly measured. It follows that closed-loop control is implemented on the joint positions only and not on the end-effector position. Indeed, the nominal position of the end-effector is determined by the position of the three joints and is derived using the direct kinematics of the robot. This results in the implementation of an open-loop control for the end-effector position that can be affected by errors since its actual and nominal positions usually differ as a consequence of modelling errors, mechanical tolerances and other disturbances.

In order to decide whether the robot performance could be considered satisfactory, an error evaluation was performed on a grid of equally spaced points in the working space. Actually, the points were located only on the horizontal plane, since this is where the most consistent errors can occur because reaching any point on the horizontal plane requires the combined action of the first two joints and these are the joints with the more complex kinematics. On the contrary, the motion along the vertical axis is driven by the third joint alone whose elongation is directly measured through a potentiometer.

About 100 equally spaced target points were used. Each point was reached several times moving from different starting points and following different trajectories. The actual position of the end-effector when the target point was nominally reached was measured with an auxiliary measuring system, based on two wires wrapped on pulleys attached to multi-turn potentiometers. Such a system measures the distance of the end-effector from two known positions where the potentiometers are fixed and enables the position of the end-effector to be derived from two simple geometrical relations. It was possible therefore to determine all errors committed by the robot comparing on a grid in the working space the nominal position of the robot with the actual one measured with the auxiliary system. A similar approach was proposed in Belforte *et al.* (1998). Such errors differ from trial to trial, and from point to point, but they are in the range of ± 26 mm. The error variability has been evaluated averaging the errors obtained reaching each target point and a moderate systematic error component has been also evidenced. In order to compensate as much as possible for the systematic error component, a calibration procedure was implemented to determine the best parameter values (lengths of the main parts of the robot) to be used when computing the kinematics of the robot. By performing a least-squares identification of a set of relevant parameters (a_2, z_0, y_0, c_0, k_1, k_2, and f_0), the optimal parameter estimates were therefore obtained, minimising the sum of the squared errors in the measured target points. After this tuning phase, the

differences between nominal and actual positions for all the tested points were smaller than 8 mm, well within acceptable operating limits. In *Fig. 7* the histogram of the absolute error is reported after the correction. Note that most of the errors are smaller than 4 mm although there is no point with an error smaller than 0·5 mm, This last value is close to the precision of the auxiliary measurement system and no errors beyond this threshold do not represent any problem.

7. Trials of agricultural operations

Besides tests and studies on the motion of the robot to evaluate the performance of such a low-cost equipment and besides the studies on procedures to take advantage of the artificial vision equipment for trajectory control, the robot was also used to test agricultural operations. The aim was not to perform extensive tests on several agricultural operations, that will be carried on in further work, but rather to demonstrate that it is actually possible to carry on important agricultural tasks with this simple machine. Two test tasks were carefully chosen to show some extras that can be offered by the machine since both tasks can be hardly conducted by human operators. The first task consists of precision spraying for cyclamens. This crop frequently needs treatment, but, to be really useful, the spraying should occur within and under the leaf canopy of the plant since the pests to be targeted live under the leaves. To spray the cyclamens efficiently they should be sprayed one by one, properly positioning the spraying nozzle. This indeed is practically impossible with human operators when the number of plants to be processed is huge as it is usually in dedicated enterprises. The task, however, can be done by a robot that do not lose concentration during the operations and can work indefinitely day and night.

The second task considered consisted in precision fertilisation, delivering to each pot a pre-defined amount of granular fertiliser that, in the robot application can be easily adjusted to the specific needs of each single plant. This last feature is related to the fact that the dispenser mainly comprises a rotary vane valve actuated by a step motor.

Both tasks were implemented and successfully carried on in the greenhouses of the Centro Regionale di Sperimentazione e Assistenza Agricola (CeRSAA) situated in Albenga (Italy). *Figure 8* shows one phase of precision spraying performed by the robot on each plant in the benches that the belt-conveyor brings into the working volume of the machine. The machine is rather slow (about 7 pots per minute), but speed requirements were not a priority since they can be left for a future engineering phase. The detailed view of the

Fig. 8. Detailed view of the head of the manipulator, with the camera, the laser pointer and the illumination system, in the case of under leaf spraying on cyclamen

Fig. 9. Detailed view of the head of the manipulator equipped with the dispenser of granular fertilisers

dispenser for granular fertiliser is shown in *Fig. 9*. For this second application the machine speed was of 8 pots per minute.

8. Conclusions and future developments

Automation of agricultural processes will be the challenge of the next years, especially in structured environments such as greenhouses. The preliminary experimentation carried on with the prototypal robot presented in this paper has shown that automated agricultural tasks can be satisfactorily performed. Two operations—precision spraying and precision fertilisation—have been considered in this preliminary study.

They can be continuously carried on by the robot for virtually unlimited periods while they are unaffordable for human operators. Indeed the relatively low productivity of the robot prototype (in the range of 400–500 plants per hour) is unsatisfactory for commercial production, but it is not critical for research and study. The present robot working capacity is mainly related to the use of in-home available components for the prototype construction and could be consistently increased in an engineering stage.

To reach the objective of an efficient automation, the next step consists of developing tools and algorithms for managing the largest possible number of different agricultural tasks to reach the stage in which the robot can perform (almost) all the operations needed in a complete cultivation cycle.

Acknowledgements

The authors would like to thank National Instruments Italy s.r.l., Agricontrol s.n.c. and CeRSAA for their support to this research project. Authors would like also to thank Stefano Tribocco, Paolo Pezzuto, Giorgio Perin and Guarino Benvegnù that collaborated to the construction of the robot. This work was partially granted by a research program launched in the framework of the Italian National Coordinated Programs, supported by MIUR, the Italian Ministry for Education, University and Research and MURST ex 60% founds.

References

Åstrand B; Baerveldt A J (2002). An agricultural mobile robot with vision-based perception for mechanical weed control. Autonomus Robots, **13,** 21–35

Bak T; Jakobsen H (2004). Agricultural robotic platform with four wheel steering for weed detection. Biosystems Engeneering, **87**(2), 125–136, doi:10.1016/j.biosystemseng.2003.10.009

Belforte G; Dabbene F; Gay P (1998). Optimal design of a measurement system for the calibration of a flexible pneumatic actuator. Proceedings of the IEEE Conference on Control Application, Trieste, Italia, pp 532–536

Benson E R; Reid J F; Zhang Q (2003). Machine vision-based guidance system for an agricultural small-grain harvester. Transactions of the ASAE, **46**(4), 1255–1264

Blasco J; Alexios N; Roger J M; Rabatel G; Moltò E (2002). Robotic weed control using machine vision. Biosystems Engeneering, **83**(2), 149–157

Chateau T; Debain C; Collange F; Trassoudaine L; Alizon J (2000). Automatic guidance of agricultural vehicles using a laser sensor. Computers and Electronics in Agriculture, **28,** 243–257

Chen B; Tojo S; Watanabe K (2003). Machine vision based guidance system for automatic rice transplanters, Transactions of the ASAE, **19**(1), 91–97

Cho S I; Chang S J; Kim Y Y (2002). Development of a three-degrees-of-freedom robot for harvesting lettuce using machine vision and fuzzy logic control. Biosystems Engineering, **82**(2), 143–149

Denavit J; Hartemberg R S (1955). A kinematic notation for lower-pair mechanism based on matrices. American Society of Mechanical Engineering Journal of Applied Mechanics, **22,** 215–221

Gay P; Giglio A (2003). Artificial vision for the control of agricultural robots, Proceedings of the 30th CIOSTA Conference, Grugliasco, 22–24 September, pp 296–307

Hague T; Marchant J A; Tillet N D (2000). Ground based sensing system for autonomous agricultural vehicles. Computers and Electronics in Agriculture, **25,** 11–28

Harper N; Mc Kerrow P P (2001). Recognising plants with ultrasonic sensing for mobile robot navigation. Robotics and Autonomous System, **34,** 71–82

Hague T; Tillet N D (1996). Navigation and control of an autonomous horticultural robot. Mechatronics, **6**(2), 165–180

Jimenez A R; Ceres R; Pons J L (1999). A machine vision system using a laser radar applied to robotic fruit harvesting. Proceedings of the IEEE Workshop on Computer Vision Beyond the Visible Spectrum: Methods and Applications, 21–22 June 1999, pp 110–119, doi:10.1109/CVBVS.1999.781100

Kassler M (2001). Agricultural automation in the new millennium, Computers and Electronics in Agriculture, **30,** 237–240

Kise M; Zhang Q; Rovira Màs F (2005). Stereovision-based crop row detection method for tractor-automated guidance. Biosystems Engineering, **90**(4), 357–367

Kondo N; Ting K C (1998). ASAE, St Joseph, MI, USA

Kondo N; Monta M (1999). Strawberry harvesting robots. ASAE/CSAE-CGR Annual International Meeting, Toronto, Canada. ASAE Paper No. 99–3071

Mandow A; Gòmez de Gabriel J M; Martínez J L; Munoz V F; Ollero A; García-Cerezo A (1996). The autonomous mobile robot AURORA for greenhouse operation. IEEE Robotics & Automation Magazine**,** 18–28

Marchant J A; Hague T; Tillet N D (1997). Row-following accuracy of an autonomous vision-guided agricultural vehicle. Computers and Electronics in Agriculture, **16,** 165–175

Monta M; Kondo N; Shibano Y (1995). Agricultural robot in grape production system, Proceedings of the IEEE International Conference on Robotics and Automation, **3,** 21–27 May, 2504–2509

Paice M E R; Miller P C H; Bodle J D (1995). An experimental sprayer for the selective application of herbicides. Journal of Agricultural Engineering Research, **60,** 107–116

Peterson D L; Bennedsen B S; Anger W C; Wolford S D (1999). A systems approach to robotic bulk harvesting of apples. Transactions of the ASAE, **42**(4), 871–876

Qiao J; Sasao A; Shibusawa S; Kondo N; Morimoto E (2005). Mapping yield and quality using the mobile fruit grading robot. Biosystems Engineering, **90**(2), 135–142, doi:10.1016/j.biosystemseng.2004.10.002

Reed J N; Miles S J; Butler J; Baldwin M; Noble R (2001). Automatic mushroom harvester development, Journal of Agricultural Engineering Research, **78**(1), 15–23

Rovia-Màs F; Zhang Q; Kise M (2004). Stereo vision navigation of agricultural tractor in structure fields. EurAgEng Paper No. 163, AgEng 2004 International Conference, Leuven, Belgium, 12–16 September

Ryu K H; Kim G; Han J S (2001). Development of a robotic transplanter for bedding plants, Journal of Agricultural Engineering Research, **78**(2), 141–146

Sanders K F (2005). Orange harvesting systems review. Biosystems Engineering, **90**(2), 115–125, doi:10.1016/j.biosystemseng.2004.10.006

Sandini G; Buemi F; Massa M; Zucchini M (1990). Visually guided operations in greenhouse. Proceedings of the IEEE International Workshop on intelligent Robots and Systems IROS '90, pp 279–285

Sarig Y (1993). Robotic of fruit harvesting: a state-of-the-art review, Journal of Agricultural Engineering Research, **54,** 265–280

Tai Y W; Ling P P; Ting K C (1994). Machine vision assisted robotic seedling transplanting. Transactions of the ASAE, **37**(2), 661–667

Thuilot B; Cariou C; Cordesses L; Martinet P (2001). Automatic guidance of a farm tractor along curved paths, using a unique CP-DGPS. Proceedings of the IEEE/RSJ International Conference on Intelligent Robots and Systems, vol 2, 29 October -3 November, pp 674–679

Tian L; Reid J F; Hummel J W (1999). Development of a precision sprayer for site-specific weed management. Transactions of the ASAE, **42**(4), 893–900

Tillett N D (1991). Automatic guidance sensor for agricultural field machine. Journal of Agricultural Engineering Research, **50,** 167–187

Tillett N D (1993). Robotic manipulators in horticulture: a review, Journal of Agricultural Engineering Research, **55,** 89–105

Tillett N D; Hague T (1999). Computer-vision-based hoe guidance for cereals—an initial trial. Journal of Agricultural Engineering Research, **74,** 225–236

Tillett N D; Hague T; Marchant J A (1998). A robotic system for plant-scale husbandry. Journal of Agricultural Engineering Research, **69,** 169–178

Tillet N D; Hague T; Miles S J (2002). Inter-row vision guidance for mechanical weed control in sugar beet. Computers and Electronics in Agriculture, **33,** 163–177

Van Henten E J; Hemming J; Van Tuijl B A J; Kornet J G; Meuleman J; Bontsema J; Van Os E A (2002). An autonomous robot for harvesting cucumbers in greenhouses. Autonomous Robots, **13,** 241–258

Van Henten E J; Hemming J; Van Tuijl B A J; Kornet J G; Bontsema J; Van Os E A (2003). Field test of an autonomous cucumber picking robot. Biosystem Engineering, **86**(3), 305–313

Van Henten E J; Van Tuijl B A J; Hoogakker G J; Van Der Weerd M J; Hemming J; Kornet J G; Bontsema J (2004). An autonomus robot for de-leafing cucumber plants grown in a high-wire cultivation system. Biosystems Engineering, **94**(3), 317–323

Appendix A

Given the parameters of the links reported in Table 1, the quaternion transformation matrices can be derived as follows

$$\boldsymbol{A}_{0,1} = \begin{bmatrix} 1 & 0 & 0 & 0 \\ 0 & 1 & 0 & 0 \\ 0 & 0 & 1 & d_1 \\ 0 & 0 & 0 & 1 \end{bmatrix} \quad \boldsymbol{A}_{1,2} = \begin{bmatrix} \cos\theta_2 & -\sin\theta_2 & 0 & a_2\cos\theta_2 \\ \sin\theta_2 & \cos\theta_2 & 0 & a_2\sin\theta_2 \\ 0 & 0 & 1 & 0 \\ 0 & 0 & 0 & 1 \end{bmatrix}$$

$$\boldsymbol{A}_{2,3} = \begin{bmatrix} 0 & 1 & 0 & 0 \\ 1 & 0 & 0 & 0 \\ 0 & 0 & -1 & -d_3 \\ 0 & 0 & 0 & 1 \end{bmatrix}$$

Finally, the complete transformation matrix $\boldsymbol{A}_{0,3} = \boldsymbol{A}_{0,1}\,\boldsymbol{A}_{1,2}\,\boldsymbol{A}_{2,3}$ is

$$\boldsymbol{A}_{0,3} = \begin{bmatrix} 1 & 0 & 0 & 0 \\ 0 & 1 & 0 & 0 \\ 0 & 0 & 1 & d_1 \\ 0 & 0 & 0 & 1 \end{bmatrix} \begin{bmatrix} \cos\theta_2 & -\sin\theta_2 & 0 & a_2\cos\theta_2 \\ \sin\theta_2 & \cos\theta_2 & 0 & a_2\sin\theta_2 \\ 0 & 0 & 1 & 0 \\ 0 & 0 & 0 & 1 \end{bmatrix} \times \begin{bmatrix} 0 & 1 & 0 & 0 \\ 1 & 0 & 0 & 0 \\ 0 & 0 & -1 & -d_3 \\ 0 & 0 & 0 & 1 \end{bmatrix}$$

i.e.

$$\boldsymbol{A}_{0,3} = \begin{bmatrix} 0 & 0 & -1 & -d_3 \\ -\sin\theta_2 & \cos\theta_2 & 0 & a_2\cos\theta_2 \\ \cos\theta_2 & \sin\theta_2 & 0 & a_2\sin\theta_2 + d_1 \\ 0 & 0 & 0 & 1 \end{bmatrix}$$